DOI:10.1190/1.3627938

Processing 3-D dual-sensor towed streamer data using local crossline slowness estimates

Tilman Klüver and Anthony Day, PGS*

Summary

Dual-sensor towed streamer data can be decomposed into data containing only the up-going (or down-going) part of the recorded total wave fields. The separation into up-going and down-going parts depends on the emergence angle of the wave fronts at the receiver and is therefore commonly applied in the plane wave domain. Large separation of the small number of streamers requires extensive data reconstruction to provide the aperture and receiver spacing necessary for proper 3-D plane wave decomposition. Here, a new method is presented to remove the necessity for data reconstruction. It is based on multiple processing of single streamer data sets using crossline slowness estimates. 4-D differences to a conventional hydrophone-only base survey are reduced when the new method is applied compared to differences observed when the crossline dip component is neglected in dual-sensor data processing.

Introduction

Dual-sensor towed streamer data, which constitutes of measurements of both the pressure and the vertical component of particle velocity, can be decomposed into data containing only the up-going (or down-going) part of the recorded total wave fields. The receiver-side ghost due to reflection of the up-going wave field at the sea surface can thus be removed. Consequently, the seismic bandwidth is significantly increased which yields large advantages in seismic processing, imaging and interpretation.

The separation of dual-sensor data into up-going and down-going constituents depends on the emergence angle of the wave fronts at the receiver and is therefore commonly applied in the plane wave domain. Reliable estimates of this angle can only be obtained with sufficiently dense receiver spreads. This is not necessarily the case in towed streamer acquisition, especially in the cross-streamer direction. Large separation of the small number of streamers requires extensive data reconstruction to provide the aperture and receiver spacing necessary for proper 3-D plane wave decomposition.

Here, a new method is presented which overcomes the need for relatively costly data reconstruction. Each streamer is processed independently which makes the method fast. The accuracy of the method is demonstrated using field data examples. One data example is a 4-D comparison between a conventional pressure-only base survey and a dual-sensor monitor survey acquired in shallow water in the North Sea. In the shallow part of the section, where crossline components of the horizontal slowness are largest, the method reduces the 4-D difference compared to differences observed when the crossline dip component is neglected in dual-sensor data processing.

Method

Dual-sensor wavefield separation as described in Carlson et al. (2007) is performed by combining a scaled version of the vertical particle velocity record with the hydrophone record yielding

$$P^{up} = \frac{1}{2}\left(P - FV_z\right) \quad \text{and} \quad P^{down} = \frac{1}{2}\left(P + FV_z\right),$$

where F denotes a frequency and wavenumber dependent scaling filter:

$$F(\omega, k_x, k_y) = \frac{\rho\omega}{k_z}, \quad \text{with} \quad k_z = \sqrt{\left(\frac{\omega}{c}\right)^2 - k_x^2 - k_y^2}\,.$$

A derivation of this filter is given by Amundsen (1993). In the above formulae k_x, k_y and k_z denote the three components of the angular wavenumber vector, ω denotes angular frequency, ρ and c are the density of water and the acoustic wave propagation velocity in water, respectively. The low frequency part of the vertical particle velocity record tends to be contaminated noise. Therefore, the low frequency part is built from the pressure record according to

$$V_z(\omega, k_x, k_y \mid z_R) = -F^{-1}\left[\frac{1 + e^{-i2k_z z_R}}{1 - e^{-i2k_z z_R}}\right] P(\omega, k_x, k_y \mid z_R),$$

where z_R denotes streamer depth. This equation describes the deghosting of the hydrophone record and imposition of the particle velocity ghost function onto it, along with the application of the inverse scaling filter and a sign correction. Once separated, up-going and down-going fields can be extrapolated to a different datum, e.g., to match a total pressure base survey in a 4-D project.

All processing steps mentioned above depend on the vertical component of the wavenumber vector. Without extensive data reconstruction in crossline direction, too small a number of samples are input to the 3-D Fourier transform to provide sufficient crossline dip resolution in plane-wave decomposition for successful application of the equations in the frequency wavenumber domain (Klüver et al., 2009). Furthermore, the crossline wavenumber axis is heavily aliased due to large streamer separation.

Assuming the crossline component of the slowness vector is known for the data, these problems can be overcome.

DOI:10.1190/1.3627938

The crossline component of the wavenumber vector is replaced by the product of angular frequency and crossline component of the slowness vector. The vertical wavenumber no longer depends on k_y and all dual-sensor processing steps can be applied in a 3-D sense using 2-D Fourier transforms of well sampled, single streamer subsets of 3-D shot records. There is, of course, not just one crossline dip in a shot record. Therefore, processing is repeated with different crossline slowness values covering the expected range. The final section is composed sample-by-sample, interpolating the two processing results closest to the actual crossline slowness value at the sample under consideration. The difference between neighbouring crossline slowness values for which processing is performed, is chosen such that the scaling factor F changes by a small, user-defined amount, e.g. 5 percent.

The actual crossline slowness values for each sample can be determined in various ways. In complex cases, dip measurement using, e.g., semblance analysis is a possibility. In the examples shown later, shallow water North Sea data with a more or less 1-D structure, crossline slowness values are determined using a representative NMO velocity function and geometry information. Fomel (2005) derived a relationship between NMO velocity and horizontal slowness

$$\frac{1}{v_{NMO}^2} = p(t,h)\frac{t}{2h},$$

where h denotes half-offset, which is used to determine the actual slowness value at every sample. Inline and crossline components are determined from this total value using inline and crossline offset and assuming radial symmetry:

$$p_x(t,h) = \frac{h_x}{|h|}p(t,h) \text{ and } p_y(t,h) = \frac{h_y}{|h|}p(t,h) \cdot$$

In case of data extrapolation to a different datum, the crossline slowness values are needed at the output level. This is achieved by converting the NMO velocity to interval velocity, stripping off (or adding) a part of the water column, and converting back to NMO velocity.

A typical crossline slowness section for a 3D shot record of the North Sea data set used below is displayed in Figure 1. Crossline slowness values are smaller for inner cables. Generally, the magnitude of crossline slowness values decreases rapidly with offset and, due to ray-bending, also with depth. From this figure, it is clear that, for geological settings as considered here, neglecting crossline dips in dual-sensor data processing leads to measurable errors only for small offsets and in the very shallow on outer cables.

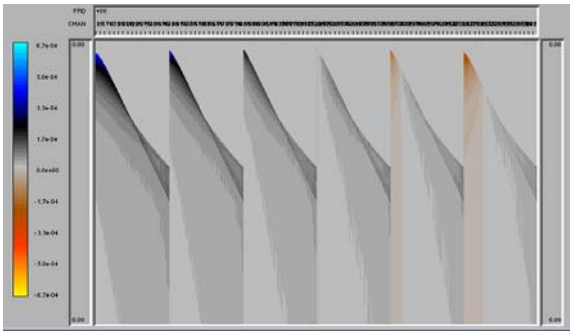

Figure 1: Crossline slowness section derived from a NMO velocity function for a 3-D shot record with six streamers from a shallow water North Sea data set. The colour bar covers the slowness value range from -0.000667 to 0.000667.

Data example

A dual-sensor towed streamer data set was used to demonstrate the method. The data were acquired in 2009 in the North Sea with six dual-sensor streamers at 15 m depth. To verify the method, wavefield separation was performed and the up-going and down-going pressure fields independently extrapolated to the surface where their sum, i.e. the total pressure, should vanish. This test was performed for an outer cable where the largest crossline slowness values are expected. Effects are largest in the shallow as the crossline slowness decreases with depth for a fixed crossline offset in an approximately 1-D medium. This is reflected in the crossline slowness section shown in Figure 1. As a second test, the data set was compared in a 4-D sense to a conventional, hydrophone-only base survey acquired with 8 m streamer depth a couple of months earlier (Day et al., 2010). A single NMO velocity function representative for the entire survey was used to estimate crossline slowness values.

Figure 2 shows the total pressure at the surface for selected crossline sections obtained with wavefield separation and redatuming neglecting crossline dips and with the method presented here. There is a clear footprint of residual energy when crossline dips are neglected (marked in Figure 3 for one crossline section). The residuals rapidly decrease with increasing time. The residuals occur at inline positions where predominantly outer streamers contribute to the stack, i.e. they are about halfway between the sail lines of the vessel. These residuals are significantly reduced when crossline dips are taken into account in wavefield separation and redatuming using the method presented here. At the same time, inline positions where mostly inner streamers contribute as well as later times with smaller crossline dips stay unchanged. This proves the ability of the proposed method to take crossline dips into account in

DOI:10.1190/1.3627938

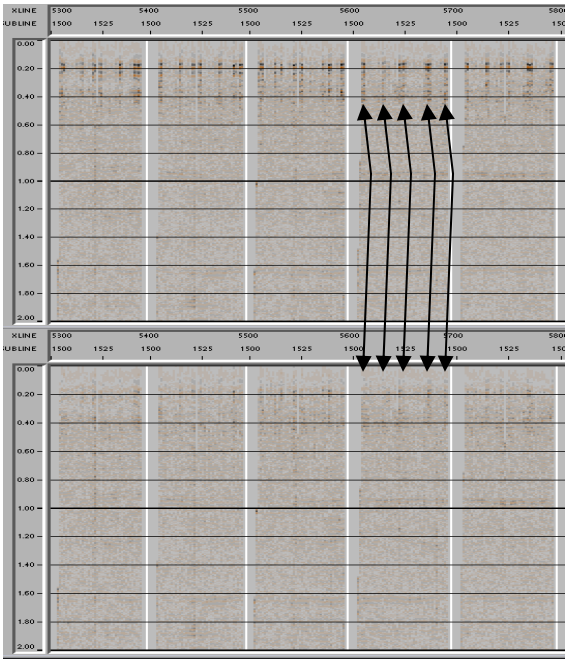

Figure 2: Selected stacked crossline sections of total pressure at the surface. Top: processing without taking into account crossline dips. Bottom: processing with the proposed method. Note the reduced footprint of residual energy.

dual-sensor data processing of single streamer subsets of 3-D shot records.

In a second test, the data is compared in 4-D sense to a base survey acquired with hydrophone-only streamers. The 4-D processing sequence comprises basic noise removal, deterministic matching of the two recording systems, and tidal static corrections, i.e. the 4-D comparison is made very early in the processing sequence where the 4-D difference is still high. As shown by Day et al. (2010) the 4-D difference decreases significantly towards the end of the processing sequence. The dual-sensor data is used to reconstruct the total pressure field at 8 m cable depth to match the recording depth of the conventional base survey. Figure 3 shows selected crossline sections of the 4-D difference between monitor and base survey. Note that the display gain is exaggerated to emphasize the 4-D differences, the stack itself would be heavily over-clipped as its amplitudes are significantly larger than the 4-D differences. When crossline dips are neglected in the processing of the dual-sensor data, the 4-D difference shows the same footprint in the shallow already observed in the comparison at the free surface: the 4-D difference is larger for inline positions where mostly outer streamers contribute to the stack. The effect is expected to be significantly smaller than in Figure 2 since the redatuming

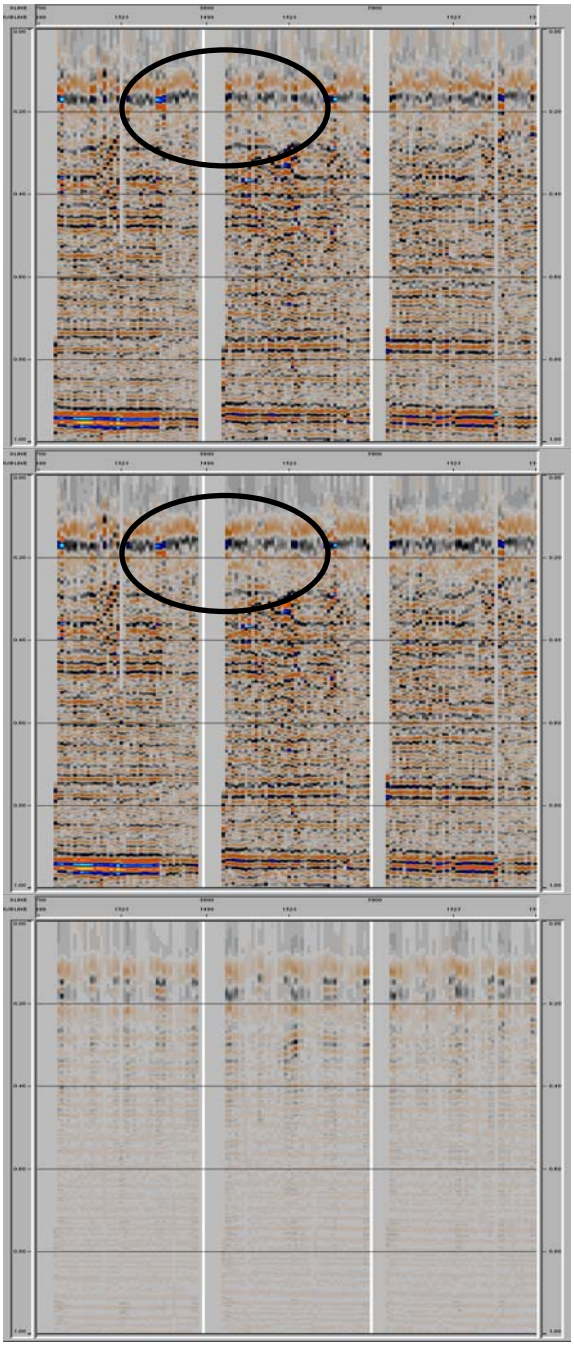

Figure 3: From top to bottom: 4-D difference after processing neglecting crossline dips, 4-D difference after processing with the proposed method, and difference between the two 4-D difference stacks. Improvements in the 4-D difference in the shallow are highlighted. The display gain is exaggerated to emphasize the differences.

DOI:10.1190/1.3627938

distance is approximately half. Whilst the footprint is generally small everywhere, especially deep in the section, application of the proposed method reduces the footprint as highlighted in Figure 3. 4-D differences for outer streamers are reduced to the same level observed at inline positions where mostly inner streamers contribute to the stack. These inline positions have the same 4-D difference for both processing methods. This pattern is most evident looking at the difference between the two 4-D difference stacks. Note that changes in the 4-D difference are small compared to the 4-D difference itself.

The effect is more evident in 4-D attributes as shown in Figure 4 for two different time windows. In the shallow window where crossline dip effects are largest, the footprint in the normalized RMS amplitude difference, time shift, and phase rotation is reduced when the proposed method is used. The footprint is most obvious in the difference between the attribute panels. At inline positions where mostly inner streamers contribute to the analysed stacks, the 4-D difference remains unchanged. Looking at the deeper window reveals that at typical target depths, crossline dip effects practically vanish for geological settings as considered here.

Conclusions

A new method for processing 3-D dual-sensor towed streamer data has been presented which allows us to take crossline dip effects into account without extensive data regularization as necessary for proper 3-D plane wave decomposition. Each streamer is processed independently making the method effective and flexible. Final outputs are composed using crossline slowness values derived for each sample. Even crossline slowness estimates derived from a single NMO velocity profile representative for the data set chosen in the example lead to 4-D improvements in the form of attributes which are independent of crossline dip effects. This indicates the robustness of the method.

Acknowledgments

The authors are grateful to many colleagues for valuable discussions and suggestions. The authors thank PGS for permission to publish this work.

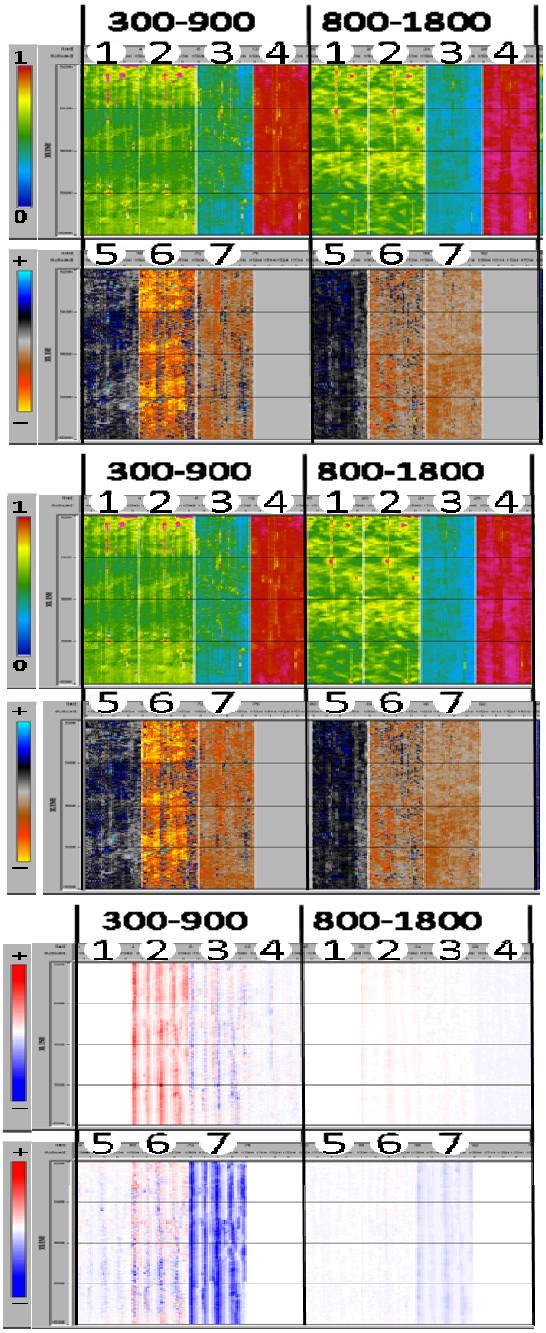

Figure 4: 4-D attribute panels for two different time windows. Top: processing neglecting crossline dips. Centre: processing with the proposed method. Bottom: difference between 4-D attributes (3-D minus 2-D). Attributes for each time window are RMS base (1), RMS monitor (2), normalized RMS difference (3), and cross-correlation (4), time shift (5), phase rotation (6), and RMS ratio (6).

DOI:10.1190/1.3627938

EDITED REFERENCES

Note: This reference list is a copy-edited version of the reference list submitted by the author. Reference lists for the 2011 SEG Technical Program Expanded Abstracts have been copy edited so that references provided with the online metadata for each paper will achieve a high degree of linking to cited sources that appear on the Web.

REFERENCES

Amundsen, L., 1993, Wavenumber-based filtering of marine point-source data: Geophysics, **58**, 1335–1348, doi:10.1190/1.1443516.

Carlson, D., A. Long, W. Söllner, H. Tabti, R. Tenghamn, and N. Lunde, 2007, Increased resolution and penetration from a towed dual-sensor streamer: First Break, **25**, 71–77.

Day, A., M. Widmaier, T. Høy, and B. Osnes, 2010, Time-lapse acquisition with a dual-sensor streamer over a conventional baseline survey: 80th Annual International Meeting, SEG, Expanded Abstracts, 4180–4184.

Fomel, S., 2005, Velocity-independent time-domain seismic imaging using local event slopes: 75th Annual International Meeting, SEG, Expanded Abstracts, 2269–2272.

Klüver, T., P. A. Aaron, D. H. Carlson, A. Day, and R. van Borselen, 2009, A robust strategy for processing 3D dual-sensor towed streamer data: 79th Annual International Meeting, SEG, Expanded Abstracts, 3088–3092.